

# A Multiplicative Cancellation Approach to Multipath Suppression in FM Radio

Thomas J. Moir · Archibald M. Pettigrew

© Springer Science+Business Media New York 2013

**Abstract** The deceptively simple problem of a single inverted reflection in ordinary frequency modulated (FM) radio is considered. It will be shown that this problem has been overlooked in the literature and causes major breakdown in reception. The problem is known as suppressed-carrier AM-FM (SCAM-FM) and is totally destructive to the received signal. We examine the theory and practical measurements of SCAM and show a solution for reducing its effect.

**Keywords** FM · Frequency-modulation · Multipath interference · Amplitude-locked loop · Phase locked loop

## 1 Introduction

There are several breakdown mechanisms in ordinary FM mobile radio. The literature explains such effects as threshold (where the carrier to noise ratio drops below an acceptable level), co-channel interference (where more than one transmitter is using the same carrier frequency) and multi-path interference (where a modulated signal is reflected off a nearby building or hill). In most cities, the transmitter power is more than adequate to cope with any problems with threshold and co-channel interference is rarer still since commercial broadcaster are at least aware of this problem and space the transmitters and carrier frequencies accordingly. This leaves the most common problem which is multi-path reflections.

Multipath interference in FM was first analysed by Corrington [1], and is most often found in mobile environments as shown in Fig. 1. The combination of the original FM signal plus a major (and probable many minor) reflections off buildings cause distortion to the demodulated baseband signal which is seen as large spikes [1].

T. J. Moir (✉)

School of Engineering, AUT University, St Pauls Street, Auckland, New Zealand  
e-mail: Tom.Moir@aut.ac.nz

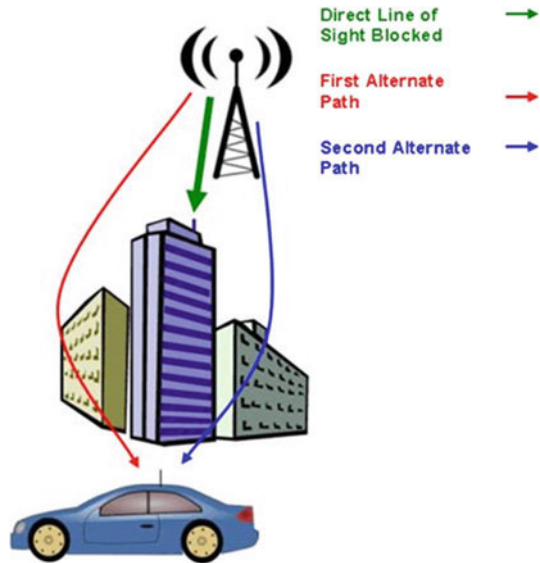
A. M. Pettigrew

Ampsys Electronics Ltd., 69 Haco Street, Largs, Scotland

Wondershare PDF Editor

Springer

**Fig. 1** Multipath interference in a car environment



22 Since the Corrington paper was published there have been several attempts at reducing  
 23 the effects of multipath interference. Perhaps one of the most commonest approaches in the  
 24 literature is to use adaptive equalization [2,3]. Such approaches have proven successful in  
 25 cases where the reflection is not too severe. Similarly, adaptive filtering methods can be used  
 26 and combined with so-called “diversity” receivers, whereby improvement is sought with the  
 27 complexity of using several antennas and receivers [4,5]. One of the earliest approaches was  
 28 to use the constant modulus algorithm (CMA), but this was found not to respond well to  
 29 rapid fading [6].

30 The approach used here also relies on the fact that for ideal FM transmission, the modulus  
 31 of the waveform will be a constant. However, we consider a special case of multi-path that has  
 32 been overlooked in the current theory, one single ‘mirror’ reflection with the same amplitude  
 33 but inverted phase. During short periods of time the carrier disappears completely for this  
 34 particular case (infinite fading). Maintaining lock with a phase-locked-loop is particularly  
 35 difficult but is accomplished with the help of an amplitude-Locked-Loop [7]. This has been  
 36 illustrated elsewhere for synchronous demodulation of double-sideband-suppressed carrier  
 37 signals [8]. In reference [8] it is shown that a phase-locked loop cannot remain locked during  
 38 periods of sustained absence of the carrier (that coincides with the free-running frequency of  
 39 the loop). This is because there is no power at the carrier frequency and hence no signal for  
 40 the loop to lock into. The inclusion of an amplitude-locked loop enables this problem to be  
 41 overcome long enough to sustain lock.

42 The contributions in this paper is first to define mathematically the type of interference  
 43 that occurs in multipath problems and then to devise a special signal processing (analogue or  
 44 digital) method which generates an in-phase signal which goes to zero when the interference  
 45 spike reaches its peak. This is known as a correction signal. Then by the process of multipli-  
 46 cation of the correction signal and the interference spikes caused by the process of multipath,  
 47 a significant reduction (if not total elimination in some cases) in these spikes is obtained.  
 48 This is made possible because information on the envelope of the composite FM signal plus  
 49 interference is made use of in generation of the correction signal which cancels the interfer-

ence. A number of other refinements are also used including the use of the amplitude-locked loop instead of a hard limiter. In fact the amplitude-locked loop is a crucial part of the circuit design.

## 2 The Basic Problem

Ordinary FM is defined as

$$y(t) = \cos(\omega_c t + \beta \sin(\omega_m t)) \tag{1}$$

where  $\omega_c$  is the carrier frequency,  $\beta = \omega_{pm}/\omega_m$  is the FM modulation index,  $\omega_m$  is the modulating frequency and  $\omega_{pm}$  is the peak modulation depth.

Now consider a single reflection of amplitude  $m$  (normally unity but we keep it general for the time being) delayed by delay  $\tau$  seconds and added to (1) above giving:

$$f(t) = y(t) + my(t - \tau) \tag{2}$$

$$f(t) = \cos(\omega_c t + \beta \sin(\omega_m t)) + m \cos(\omega_c(t - \tau) + \beta \sin(\omega_m(t - \tau))) \tag{3}$$

Now if this delay is assumed to be  $\tau = \pi/\omega_c$ , then without losing generality, the delay also applies when substituting  $\pi$  for  $(2n - 1)\pi$ ,  $n = 1, 2, 3, \dots$  where  $n$  is defined as the wave number. This is because in our analysis  $\sin((2n - 1)\pi) = 0$ ,  $n = 1, 2, 3, \dots$  and  $\cos((2n - 1)\pi) = -1$ ,  $n = 1, 2, 3, \dots$ . Then we can expand (3) above in two parts

$$\cos(\omega_c t + \beta \sin(\omega_m t)) = \cos(\omega_c t) \cos(\beta \sin(\omega_m t)) - \sin(\omega_c t) \sin(\beta \sin(\omega_m t)) \tag{4}$$

and

$$m \cos(\omega_c(t - \tau) + \beta \sin(\omega_m(t - \tau))) = m \cos(\omega_c t - \pi) \cos\left(\beta \sin\left(\omega_m t - \frac{\omega_m}{\omega_c} \pi\right)\right) - m \sin(\omega_c t - \pi) \sin\left(\beta \sin\left(\omega_m t - \frac{\omega_m}{\omega_c} \pi\right)\right) \tag{5}$$

Now of course  $\cos(\omega_c t - \pi) = -\cos(\omega_c t)$  and  $\sin(\omega_c t - \pi) = -\sin(\omega_c t)$

To simplify  $\cos(\beta \sin(\omega_m t - \frac{\omega_m}{\omega_c} \pi))$  first simply  $\sin(\omega_m t - \frac{\omega_m}{\omega_c} \pi)$  and note that  $\cos(\frac{\omega_m}{\omega_c} \pi) \approx 1$  since the carrier frequency will be in the region of 88–108 MHz (for broadcast quality FM) and the baseband frequency no larger than 15 kHz. For the worst case scenario this makes  $\frac{\omega_m}{\omega_c} \pi$  around  $535 \times 10^{-6}$  radians so that

$$\sin\left(\omega_m t - \frac{\omega_m}{\omega_c} \pi\right) = \sin(\omega_m t) \cos\left(\frac{\omega_m}{\omega_c} \pi\right) - \cos(\omega_m t) \sin\left(\frac{\omega_m}{\omega_c} \pi\right)$$

which is approximately

$$\sin\left(\omega_m t - \frac{\omega_m}{\omega_c} \pi\right) \approx \sin(\omega_m t) - \frac{\omega_m}{\omega_c} \pi \cos(\omega_m t)$$

Hence

$$\begin{aligned} \cos\left(\beta \sin\left(\omega_m t - \frac{\omega_m}{\omega_c} \pi\right)\right) &\approx \cos\left[\beta \sin(\omega_m t) - \beta \pi \frac{\omega_m}{\omega_c} \cos(\omega_m t)\right] \\ &= \cos(\beta \sin(\omega_m t)) \cos\left(\beta \pi \frac{\omega_m}{\omega_c} \cos(\omega_m t)\right) + \sin(\beta \sin(\omega_m t)) \sin\left(\beta \pi \frac{\omega_m}{\omega_c} \cos(\omega_m t)\right) \end{aligned}$$

82 which is approximately equal to

$$83 \quad \approx \cos(\beta \sin(\omega_m t)) + \sin(\beta \sin(\omega_m t)) \beta \pi \frac{\omega_m}{\omega_c} \cos(\omega_m t)$$

84 Similarly we have

$$85 \quad \sin\left(\beta \sin\left(\omega_m t - \frac{\omega_m}{\omega_c} \pi\right)\right) \approx \sin(\beta \sin(\omega_m t)) - \beta \pi \frac{\omega_m}{\omega_c} \cos(\beta \sin(\omega_m t)) \cos(\omega_m t)$$

86 adding all the terms in (1) gives

$$87 \quad f(t) \approx \cos(\omega_c t) \cos(\beta \sin(\omega_m t)) - \sin(\omega_c t) \sin(\beta \sin(\omega_m t)) \\ 88 \quad + m \left\{ -\cos(\omega_c t) \left[ \cos(\beta \sin(\omega_m t)) + \beta \pi \frac{\omega_m}{\omega_c} \sin(\beta \sin(\omega_m t)) \cos(\omega_m t) \right] \right. \\ 89 \quad \left. + \sin(\omega_c t) \left[ \sin(\beta \sin(\omega_m t)) - \beta \pi \frac{\omega_m}{\omega_c} \cos(\beta \sin(\omega_m t)) \cos(\omega_m t) \right] \right\} \quad (6)$$

90 For the special case of a perfect mirror reflection when  $m = 1$  the above simplifies to

$$91 \quad f(t) \approx \beta \pi \frac{\omega_m}{\omega_c} \cos(\omega_m t) [-\cos(\omega_c t) \sin(\beta \sin(\omega_m t)) - \sin(\omega_c t) \cos(\beta \sin(\omega_m t))] \quad (7)$$

92 Further simplifying

$$93 \quad f(t) \approx -\beta \pi \frac{\omega_m}{\omega_c} \cos(\omega_m t) [\sin(\omega_c t) \cos(\beta \sin(\omega_m t)) + \cos(\omega_c t) \sin(\beta \sin(\omega_m t))]$$

94 Finally we have

$$95 \quad f(t) \approx -\beta \pi \frac{\omega_m}{\omega_c} \cos(\omega_m t) [\sin(\omega_c t + \beta \sin(\omega_m t))] \quad (8)$$

96 The above equation clearly also applies when substituting  $\pi$  for  $(2n - 1)\pi$ ,  $n = 1, 2, 3, \dots$

97 This is an FM signal which is multiplied by an amplitude term  $-\beta(2n - 1)\pi \frac{\omega_m}{\omega_c} \cos(\omega_m t)$ ,  
98  $n = 1, 2, 3, \dots$  giving rise to the acronym suppressed-carrier AM-FM or SCAM-FM for short.  
99 See the simulation below. This waveform has both FM and AM and was simulated from  
100 equation (2) with  $m = n = 1$  and not from the simplified model (8) though it has the same  
101 form.

102 We may further examine the effects of this problem in the frequency domain by examining  
103 the frequency domain properties of the propagation channel. Although Fig. 2 looks like

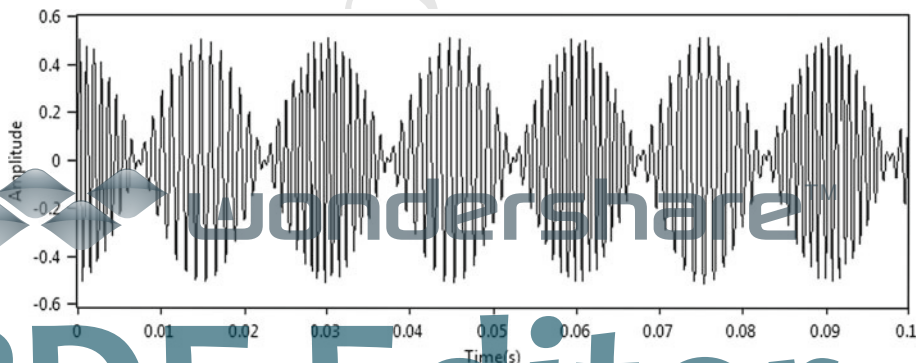


Fig. 2 A simulation of SCAM-FM

104 normal double-sideband suppressed carrier (DSSC), it should be pointed out that the above  
 105 waveform is also frequency modulated.

106 Taking Fourier transforms of (2) gives

107 
$$f(j\omega) = y(j\omega)[1 + me^{-j\omega\tau}] \tag{9}$$

108 Defining  $G(j\omega) = 1 + me^{-j\omega\tau}$  we see that the original FM signal has become convolved  
 109 (i.e. filtered) by the path transfer function  $G(j\omega)$

110 
$$f(j\omega) = G(j\omega)y(j\omega) \tag{10}$$

111 and we need only find the characteristics of  $G(j\omega)$  in order to find the frequency domain  
 112 properties of SCAM-FM. In fact  $G(j\omega)$  has a well known form when  $m=1$  and is easily  
 113 manipulated.

114 
$$G(j\omega) = 2e^{-j\omega\tau/2} [e^{j\omega\tau/2} + e^{-j\omega\tau/2}] / 2$$
  
 115 
$$= 2e^{-j\omega\tau/2} \cos(\omega\tau/2)$$

116 Now substitute  $\tau = (2n - 1)\pi/\omega_c$ ,  $n = 1, 2, 3, \dots$  and we get

117 
$$G(j\omega) = 2e^{-j\frac{(2n-1)\pi}{2}(\omega/\omega_c)} \cos\left(\frac{(2n-1)\pi}{2}(\omega/\omega_c)\right), \quad n = 1, 2, 3, \dots$$

118 The magnitude of this becomes

119 
$$|G(j\omega)| = 2 \left| \cos\left(\frac{(2n-1)\pi}{2}(\omega/\omega_c)\right) \right|, \quad n = 1, 2, 3, \dots \tag{11}$$

120 Which has an absolute valued cosine characteristic of amplitude 2 and it goes to zero at  
 121  $\omega = \omega_c$ . It has a gain of 0.707 (-3 dB down) at  $\omega = \omega_c/2$  ie half the carrier frequency. In  
 122 general zeros of the frequency response occur when

123 
$$\frac{(2n-1)\pi}{2}(\omega/\omega_c) = \frac{(2n-1)\pi}{2}, \quad n = 1, 2, 3, \dots$$

124 From which  $\omega = \omega_c$  Which gives an infinite null at the carrier frequency  $\omega = \omega_c$ . The  
 125 frequency response in Hz is illustrated in Fig. 3 below and is independent of the wave  
 126 number  $n$ .

127 We note from Fig. 3 that the dB gain is minus infinity, totally suppressing the carrier  
 128 frequency and giving rise to the typical SCAM time-domain composite carrier waveform of  
 129 Fig. 2.

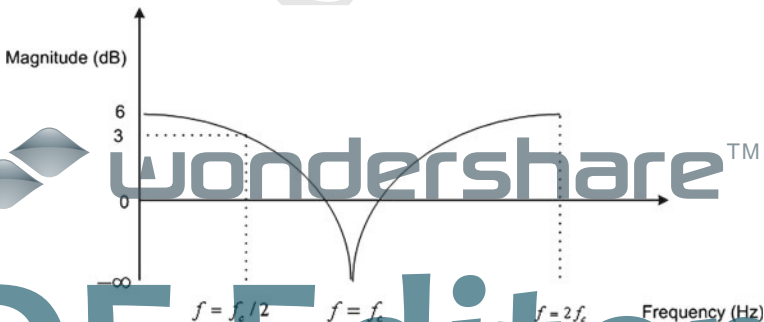


Fig. 3 Magnitude frequency response of SCAM channel

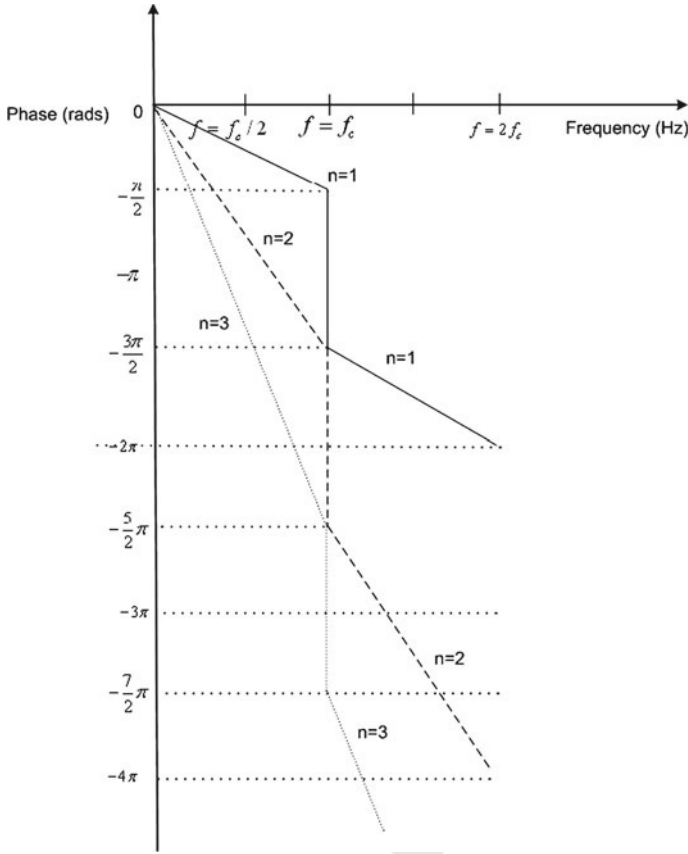


Fig. 4 Phase response of SCAM channel for  $n = 1, 2, 3$

130 The phase response is dependant on the wave number  $n = 1, 2, 3 \dots$  and is shown in Fig. 4.  
 131 Note the rapid phase change of  $-\pi$  at the notch frequency  $f_c$  for any value of  $n$ .

132 2.1 The Length of the SCAM Zone

133 Having established that a single reflection at  $180^\circ$  converts the FM carrier into the suppressed  
 134 carrier amplitude modulated function which is also frequency modulated, it is instructive to  
 135 develop a more general solution for these conditions.

136 In the interests of clarity, the value of peak deviation will be used as the modulation depth  
 137 and defined as  $\omega_{pm} = 100 \text{ kHz}$ . The carrier frequency will be defined as  $\omega_c = 100 \text{ MHz}$ .

138 From (8)



$$\begin{aligned}
 f(t) &= -\beta \pi (\omega_m / \omega_c) (\cos \omega_m t) \sin(\omega_c t + \beta \sin \omega_m t) \\
 &= -\pi (\omega_{pm} / \omega_c) (\cos \omega_m t) \sin(\omega_c t + \beta \sin \omega_m t) \\
 &= -\pi 1 / 1000 (\cos \omega_m t) \sin(\omega_c t + \beta \sin \omega_m t) \\
 &= -0.003142 (\cos \omega_m t) \sin(\omega_c t + \beta \sin \omega_m t)
 \end{aligned}$$

143 So for a carrier received at a signal strength of 1 millivolt, after the attenuation the carrier  
 144 strength will be reduced to 3.142 microvolt. If we now apply the same argument for  $3\pi$

145 
$$f(t) = (3)(-0.003142(\cos \omega_m t) \sin(\omega_c t + \beta \sin \omega_m t))$$

146 
$$f(t) = 0.009426(\cos \omega_m t) \sin(\omega_c t + \beta \sin \omega_m t)$$

147 So the signal strength increases by  $(2n-1)$  as the delay distance increases. where  $n$  is the  
 148 wave number.

149 If the delay length is not exactly  $180^\circ$ , then there will still be a certain frequency offset from  
 150 the carrier frequency where the same phase discontinuity will occur. This phase discontinuity  
 151 will occur higher and higher up the modulating cycle either in the positive or the negative  
 152 direction. When the distance is such that no discontinuity appears in the carrier then this is  
 153 the end of the SCAM zone and normal amplitude modulation returns. This point is reached  
 154 when the peak amplitude modulated signal reaches twice the value of the attenuated carrier  
 155 with pure symmetric SCAM.

156 In the case of a delay of  $180^\circ$  (1.5 m) this evaluates to  $1/1,000$  of the half wavelength or  
 157 1.5 mm. The peak-to-peak value is twice this value or 3 mm.

158 
$$\lambda_{SCAM} = \lambda_{wavelength} \omega_{pm} / \omega_c$$

159 Or more generally

160 
$$\lambda_{SCAM}(n) = (2n - 1) \lambda_{wavelength} \omega_{pm} / \omega_c \quad n = 1, 2, 3 \dots \quad (12)$$

161 There is a limit in the length of the SCAM zone that has been found experimentally

162 
$$\lambda_{SCAM}(\max) = \lambda_{wavelength} 1/1.57 \quad (13)$$

163 So, with a wavelength of 3 m the maximum length of SCAM zone can be  $3/1.57$  m or 191 cm.  
 164 at the delay distance of 751.5 m.

165 The analysis shows that there is a zone of catastrophic failure in FM reception called the  
 166 SCAM zone where the carrier is infinitely attenuated by a short distance reflection and that  
 167 this distance is a function of the ratio of the peak modulation to the carrier frequency and is  
 168 proportional to the delay distance up to about 750 m where the zone is 191 cm in length.

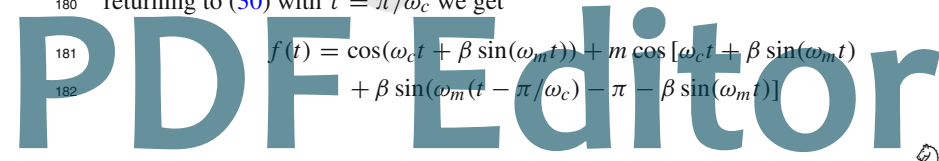
169 The distortion caused by the phase discontinuity cause severe distortion that will be  
 170 analysed in the next section.

171 **3 Demodulation in the SCAM Zone**

172 There are many issue to consider when examining how an FM demodulator will treat the  
 173 basic SCAM equation (8). For instant when a limiter is present prior to say a phase-locked-  
 174 loop and there is additive noise, the period of time when the carrier goes to zero will be  
 175 chaotic to the demodulation process. This is because a limiter will only amplify the noise  
 176 when no carrier is present. To simplify the procedure we consider the absence of noise and  
 177 that initially the phase-locked loop is ideal (i.e. it cannot respond to amplitude variations).  
 178 Equation (8) cannot be used directly in following analysis since when  $m=1$  the problem is  
 179 essentially 'singular'. Instead we must consider when  $m$  is just less than unity. Therefore  
 180 returning to (30) with  $\tau = \pi / \omega_c$  we get

181 
$$f(t) = \cos(\omega_c t + \beta \sin(\omega_m t)) + m \cos[\omega_c t + \beta \sin(\omega_m t)]$$
  
 182 
$$+ \beta \sin(\omega_m(t - \pi / \omega_c) - \pi - \beta \sin(\omega_m t)) \quad (14)$$

Author Proof



183 This we can simplify using trig identities to give

$$184 \quad f(t) = [1 + m \cos(\omega_d(t))] \cos(\omega_c t + \beta \sin(\omega_m t)) - m \sin(\omega_d(t)) \sin(\omega_c t + \beta \sin(\omega_m t)) \quad (15)$$

186 where we define

$$187 \quad \psi(t) = \beta \sin(\omega_m(t - \pi/\omega_c)) - \beta \sin(\omega_m t) - \pi \quad (16)$$

188 The Eq. (16)  $\psi(t)$  can be simplified (see Appendix 1) and will be shown to be related to twice  
189 the modulating frequency. Looking at Eq. (15) for the composite carrier we can simplify this  
190 by using the well known trig identity which follows from a right-angled triangle. We can  
191 express (15) in the simple form

$$192 \quad a \cos(x) + b \sin(x) = c \cos(x - \phi)$$

193 where

$$194 \quad \phi = \tan^{-1}[b/a], \quad c = \sqrt{a^2 + b^2}$$

195 with

$$196 \quad a = [1 + m \cos(\psi(t))], \quad b = -m \sin(\psi(t))$$

197 Hence the composite waveform (15) can be written as

$$198 \quad f(t) = r(t) \cos[\omega_c t + \beta \sin(\omega_m t) - \phi(t)] \quad (17)$$

199 The amplitude part  $r(t)$  equal to

$$200 \quad r(t) = \sqrt{1 + 2m \cos(\psi(t)) + m^2} \quad (18)$$

201 and the phase

$$202 \quad \phi(t) = \tan^{-1} \left[ -\frac{m \sin(\psi(t))}{1 + m \cos(\psi(t))} \right] \quad (19)$$

### 203 3.1 Phase-Locked-Loop Demodulated Output

204 The (ideal) phase-locked loop output  $p(t)$  is given by the derivative of the phase term of the  
205 composite waveform  $f(t)$  in (17) i.e.

$$206 \quad p(t) = \frac{d}{dt} [\omega_c t + \beta \sin(\omega_m t) - \phi(t)]$$

207 (The ideal phase-locked loop will not respond to the amplitude variations but is helped by  
208 the fact that the input composite FM signal has a constant amplitude obtained by using an  
209 amplitude-locked-loop (ALL) and not a hard-limiter)

210 The first of these derivatives becomes  $\omega_c$  which we shall ignore as this is just a dc com-  
211 ponent. The second of these derivatives is

$$212 \quad \frac{d}{dt} [\beta \sin(\omega_m t)] = \beta \omega_m \cos(\omega_m t)$$

213 and this is the ideal PLL output when there is no SCAM interference.

Author Proof

214 Since  $\tan^{-1}(-x) = -\tan^{-1}(x)$ , the final derivative is given by

$$215 \quad -\frac{d}{dt}[\phi(t)] = -\frac{d}{dt} \tan^{-1} \left[ -\frac{m \sin(\psi(t))}{1 + m \cos(\psi(t))} \right]$$

$$216 \quad = \frac{d}{dt} \tan^{-1} \left[ \frac{m \sin(\psi(t))}{1 + m \cos(\psi(t))} \right]$$

217 and after some algebra (Appendix 2) this leads to the solution

$$218 \quad -\frac{d}{dt}[\phi(t)] = \left[ \frac{m^2 + m \cos(\psi(t))}{1 + 2m \cos(\psi(t)) + m^2} \right] \beta \omega_m [\cos(\omega_m(t - \pi/\omega_c)) - \cos(\omega_m t)]$$

219 Adding all three terms reveals the solution for one reflection for a delay of  $\pi/\omega_c$  radians to  
220 be:

$$221 \quad p(t) = \frac{(1 + m \cos(\psi(t)))}{(1 + 2m \cos(\psi(t)) + m^2)} \beta \omega_m \cos(\omega_m t)$$

$$222 \quad + \frac{(m^2 + m \cos(\psi(t)))}{(1 + 2m \cos(\psi(t)) + m^2)} \beta \omega_m \cos(\omega_m(t - \pi/\omega_c)) \quad (20)$$

223 **3.2 Simplification of the Above Phase-Locked Loop Expression**

224 To simplify (20) above we need to evaluate  $\cos(\omega_m(t - \pi/\omega_c))$  on the right-hand side of the  
225 equation.

226 Expanding gives

$$227 \quad \cos(\omega_m(t - \pi/\omega_c)) = \cos(\omega_m t) \cos(\pi \omega_m/\omega_c) + \sin(\pi \omega_m/\omega_c) \sin(\omega_m t)$$

228 (since  $\pi \omega_m/\omega_c$  is a small angle we can approximate the above by using  $\cos(x) \approx 1 - \frac{x^2}{2}$   
229 and  $\sin(x) \approx x - \frac{x^3}{6}$  but we shall ignore the cubed term)

230 Hence by defining  $k = \frac{\pi \omega_m}{\omega_c}$  we have

$$231 \quad \cos(\omega_m(t - \pi/\omega_c)) = \cos(\omega_m t) - \frac{k^2}{2} \cos(\omega_m t) + k \sin(\omega_m t)$$

232 Similarly we can simplify the term  $\cos(\omega_d(t))$  by using the expression in Appendix 1.

$$233 \quad \cos(\psi(t)) \approx -1 + \frac{1}{4}(\beta k)^2 [1 + \cos(2\omega_m t)]$$

234 Now define the denominator term from the phase-locked loop output p(t) as

$$235 \quad d(t) = 1 + 2m \cos(\psi(t)) + m^2$$

236 and substituting  $\cos(\omega_d(t))$  gives

$$237 \quad d(t) \approx (1 - m)^2 + \frac{m}{2}(\beta k)^2 [1 + \cos(2\omega_m t)] \quad \text{TM}$$

238 and define the numerator term from p(t) in (20) as

$$239 \quad n(t) = m^2 + m \cos(\psi(t))$$

240 which becomes

$$241 \quad n(t) \approx m^2 - m + \frac{m}{4}(\beta k)^2 [1 + \cos(2\omega_m t)]$$



wondershare

PDF Editor

Using the above results the simplified phase-locked loop output results in

$$p(t) \approx \beta\omega_m \cos(\omega_m(t)) \left[ 1 - \frac{k^2 n(t)}{2 d(t)} \right] + k \frac{n(t)}{d(t)} \beta\omega_m \sin(\omega_m(t))$$

This is a sum of the ideal phase-locked loop output with  $m=0$  and a quadrature term which gives rise to spikes. The term in  $\frac{k^2}{2}$  can be ignored under normal conditions leaving the final simplified form:

$$p(t) \approx \beta\omega_m \cos(\omega_m(t)) + k \frac{n(t)}{d(t)} \beta\omega_m \sin(\omega_m(t)) \quad (21)$$

### 3.3 Summary of Findings

The simplified phase-locked loop output when  $m$  is just less than unity (say  $m=0.999$ ) is given by

$$p(t) \approx \beta\omega_m \cos(\omega_m(t)) + k \frac{n(t)}{d(t)} \beta\omega_m \sin(\omega_m(t))$$

where

$$k = \frac{\pi \omega_m}{\omega_c}$$

$$n(t) \approx m^2 - m + \frac{m}{4} (\beta k)^2 [1 + \cos(2\omega_m t)]$$

$$= (1 - m)^2 + (m - 1) + \frac{m}{4} (\beta k)^2 [1 + \cos(2\omega_m t)]$$

and

$$d(t) \approx (1 - m)^2 + \frac{m}{2} (\beta k)^2 [1 + \cos(2\omega_m t)]$$

This type of phase-locked loop output contains the demodulated baseband with spikes which occur at the zero-crossings of the waveform. The spikes are particularly destructive to any audio waveform.

### 3.4 Height of the Spikes

The height of the spikes follows from the expression of the phase-locked loop output. The second part of the phase-locked loop output expression is:

$$p_2(t) = k \frac{n(t)}{d(t)} \beta\omega_m \sin(\omega_m t)$$

(since the first part contains only a pure cosine wave)

The spikes have equal height and occur at the maxima and minima of the sin function. That is when  $\omega_m t = i \frac{\pi}{2}$ ,  $i = 1, 3, 5, \dots$ . Substituting this angle into  $n(t)$  and  $d(t)$  gives the magnitude

$$p_2(\max) = \left| k \frac{(1 - m)^2 + (m - 1)}{(1 - m)^2} \beta\omega_m \right|$$

$$p_2(\max) = \frac{\pi \omega_m}{\omega_c} \frac{m}{(1 - m)} \omega_{pm}$$

271 3.5 Illustrative Example

272 The commercial FM frequency band in the UK is from 88–108 MHz. Any multipath composite  
 273 carrier signal in these range of frequencies is converted down to the common intermediate  
 274 frequency of 10.7 MHz which is where the phase-locked loop is centred. For simplification  
 275 the simulation does not consider the down-conversion part of this process. Consider a single  
 276 reflection problem when the modulating frequency is 4 kHz, the peak modulating frequency is  
 277 100 kHz, the IF is 10.7 MHz and  $m = 0.999$ . For this problem  $\beta = 25(\omega_{pm} = 2\pi \times 100 \text{ kHz})$   
 278 and the theoretical phase-locked loop output when plotted is shown in Fig. 5 below.

279 The spikes are clearly visible at the zero-crossings of the demodulated signal. Note the  
 280 size of the spike relative to the signal size. The spike height follows from

$$281 \quad p_2(\text{max}) = \frac{\pi \omega_m}{\omega_c} \frac{m}{(1 - m)} \omega_{pm}$$

282 which becomes

$$283 \quad p_2(\text{max}) = 7.3717 \times 10^5$$

284 Of course in a practical circuit there will be finite bandwidth of the phase-locked loop and  
 285 a saturation limit of the amplifiers. However, any type of impulsive noise will have a wide  
 286 spectrum across the baseband spectrum and is difficult to remove. In fact it has the effect  
 287 of pushing up the noise-floor of the demodulated signal and hence reducing signal to noise  
 288 ratio.

289 4 Suppression of the Zero-Crossing Spikes

290 The method used here is quite complex but can be summarised in a simpler way by first  
 291 noticing that from Eq. (20) for the demodulated output we know that

$$292 \quad d(t) = 1 + 2m \cos(\psi(t)) + m^2$$

$$293 \quad = r^2(t)$$

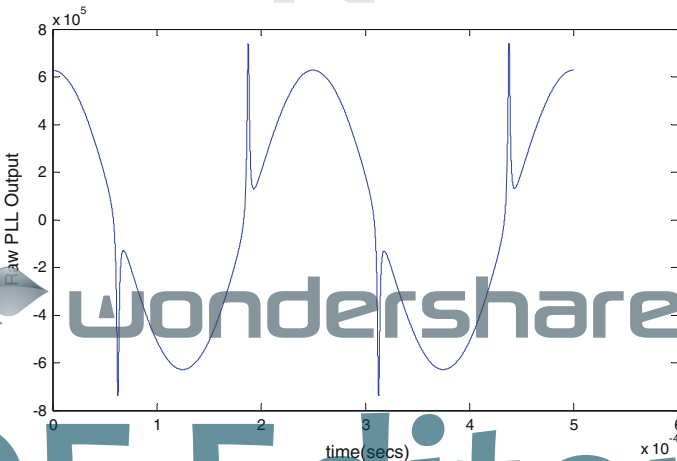
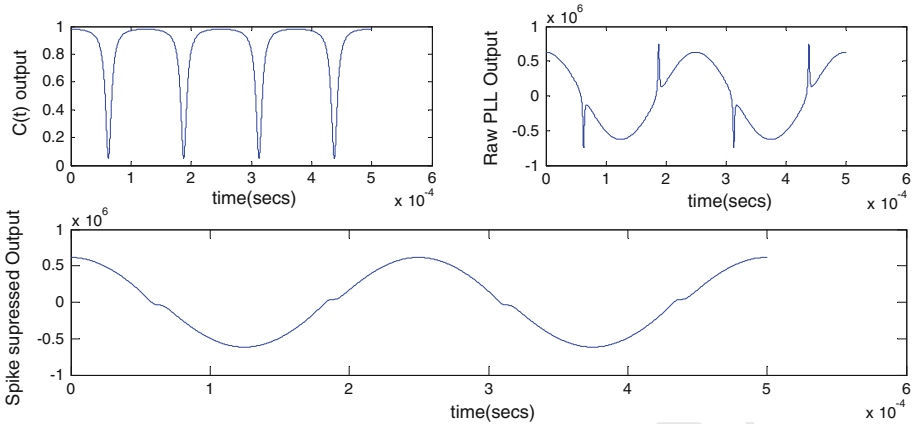


Fig. 5 Phase-locked loop output for a single 180° reflection (SCAM)

Author Proof



**Fig. 6** Shows a good cancellation effect of the spikes

294 That is, the denominator of the phase-locked loop output is exactly the same as the envelope  
 295 of the composite multipath FM waveform squared (18). Therefore it is easy to obtain a good  
 296 estimate of  $d(t)$  from the envelope of the composite FM waveform by squaring and lowpass  
 297 filtering. Once we find this we can construct a special waveform called the “correction”  
 298 waveform  $c(t)$  given by

$$299 \quad c(t) = \frac{d(t)}{[d(t) + \delta]} \quad (22)$$

300 where  $\delta$  is a small positive constant offset voltage. The waveform produces spikes which  
 301 are time-aligned to the phase-locked loop spikes (which in turn are time-aligned to the nulls  
 302 in the composite carrier waveform), except that they reach down towards zero. In fact the  
 303 narrower and closer to zero that these spikes are, the better performance, though there are  
 304 several trade-offs. When multiplied by the phase-locked loop output i.e.  $c(t)p(t)$ , the net  
 305 effect is a much purer waveform with spike suppression.

306 Using the same example 3.5 above, we can see the effect in Fig. 6 below.

307 In Fig. 6 we see the correction waveform  $c(t)$  the original phase-locked loop output with  
 308 spikes and the product  $c(t)p(t)$ .

309 It can be seen that the spikes have been totally removed except for some small residual  
 310 caused by the fact that the spikes of  $c(t)$  did not reach exactly zero. If the spikes are too wide  
 311 then there will be dead-zone at the zero-crossings of  $c(t)p(t)$ . Too narrow and there will not  
 312 be enough cancellation. The system works by simply multiplying by zero at the correct time.

313 *This is therefore a multiplicative cancellation system and not convolutive as with the case*  
 314 *of adaptive filters.*

315 The key to good cancellation is the shape of the pulse and the nearness to zero. For  
 316 example,  $\delta = 0.000018$  in Fig. 6. If the offset value is made too big then the corrective spikes  
 317 will be too fat as illustrated below in Fig. 7 when  $\delta = 0.00018$ , ten times larger.

318 When the corrective spikes are too fat this will result in distortion as shown above.

319 Likewise, if the offset is made too small then we have the situation as shown in Fig. 8  
 320 where not enough cancellation is made. The pulses do not reach zero and there are residual  
 321 spikes left.

322 To get a greater insight to the benefits, consider a 2kHz baseband signal with  $\beta = 50$ . The  
 323 demodulated signal in the frequency domain is shown before and after cancellation (Fig. 9).

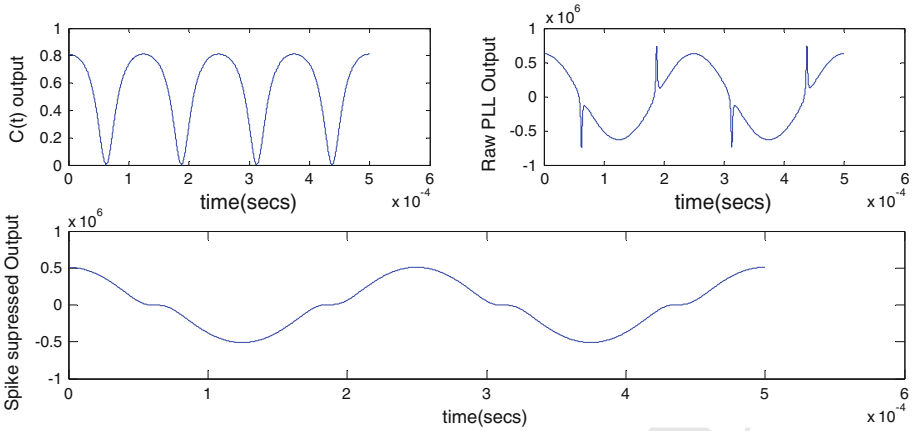


Fig. 7 Shows distortion when offset  $\delta$  is made too large

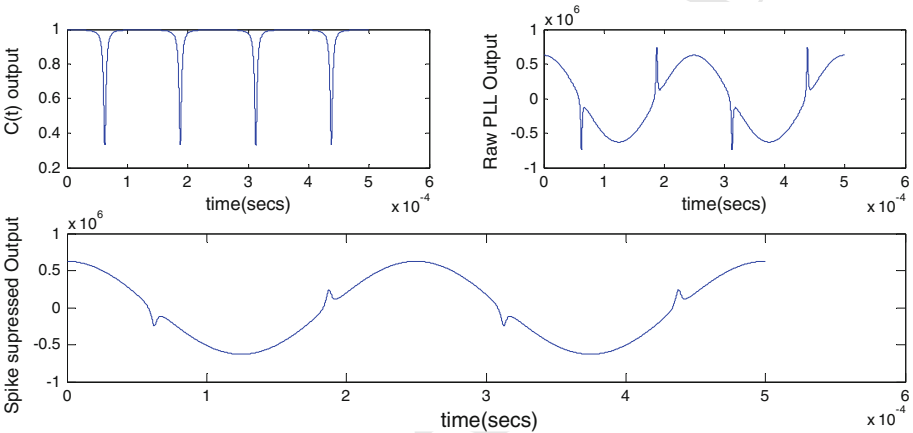


Fig. 8 Shows insufficient cancellation when offset  $\delta$  is made too small

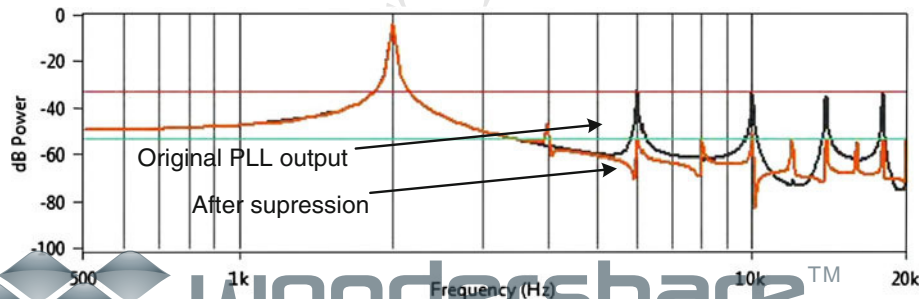


Fig. 9 Spectrum of demodulated phase-locked loop (PLL) signal before and after multipath. suppression

It can be seen that the reduction in harmonic power is by up to as much as 20 dB with detrimental effect on the spectrum of the signal itself. The suppression occurs right across the audio frequency spectrum.

327 **5 Analogue System Realization**

328 Although in theory the previous sections describe a mathematical method of removing mul-  
 329 tipath propagation, practically, the circuit realization is far from easy. Figure 10 shows the  
 330 block-diagram of the complete system working at the intermediate frequency (IF) of typical  
 331 high-quality FM.

332 The first thing which is noticeably different is that there is no hard-limiter in the system at  
 333 all. This is because the envelope needs to be preserved in order to obtain the envelope which  
 334 is squared and filtered to obtain  $d(t)$ . The envelope comes from a slow-acting automatic-gain  
 335 control circuit (AGC). The AGC output is fed into a high bandwidth amplitude-Locked Loop.  
 336 The amplitude-locked loop has been discussed elsewhere [7,8] and is a linear circuit which  
 337 flattens the envelope in a similar fashion to that of a hard-limiter but without amplifying the  
 338 zero-cross noise. In Fig. 10 the AGC has a wide dynamic range of around 120 dB whereas  
 339 the amplitude-locked loops dynamic range is around 20 dB. A hard-limiter relies on the zero-  
 340 crossings of the composite carrier waveform and can have the effect at low signal-to-noise  
 341 ratios of amplifying any additive noise. Figures 11 and 12 show the block diagrams of an  
 342 amplitude-locked-loop and a hard-limiter respectively.

343 The amplitude-locked loop works by maintaining negative feedback and high open-loop  
 344 gain around an integrator. Since the input is ac, the squarer acts as a transducer which measures  
 345 the power (or variance) in the signal and adjusts the amplitude of the output to have a carrier  
 346 power defined by the setpoint. This in turn defines the amplitude of the amplitude-locked loop

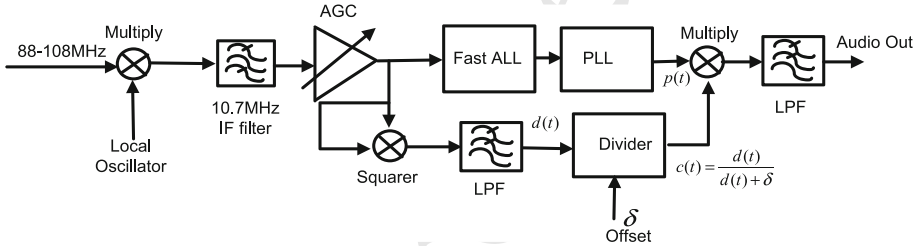
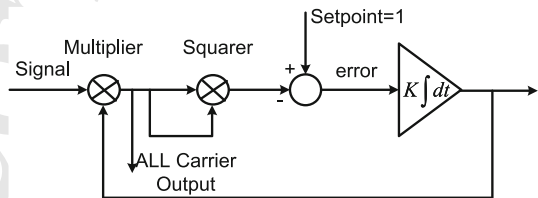


Fig. 10 Block diagram of complete demodulation process

Fig. 11 Amplitude locked-Loop



Wondershare™  
 PDF Editor  
 Springer

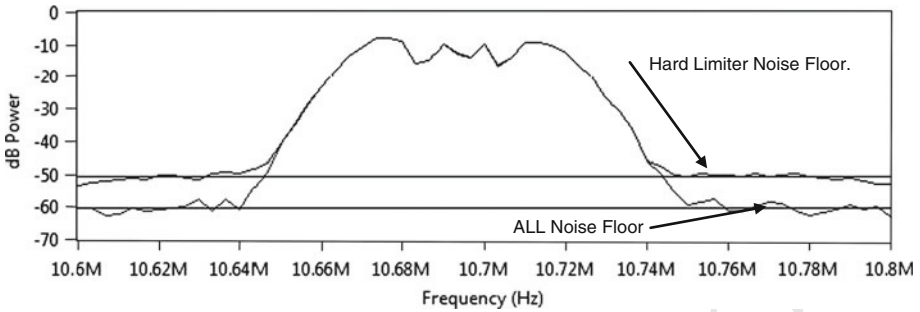


Fig. 13 Comparison of carrier amplitude-locked loop (ALL) and hard limiter noise floor

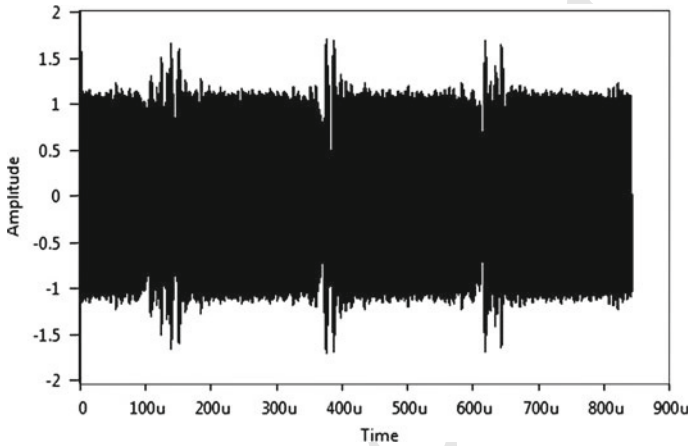


Fig. 14 Amplitude locked-loop recovered carrier

347 output which consists of a constant amplitude carrier. Of course if there are gaps in the carrier  
 348 waveform where the carrier goes to zero (as is the case with multipath), then the amplitude-  
 349 locked loop does not attempt to amplify the noise up to the same level as the envelope (as  
 350 with an AGC). Instead, it jumps “out of lock” in a similar fashion to that of its dual circuit,  
 351 the phase-locked-loop. This is a desirable property unlike the hard-limiter of Fig. 12 which  
 352 will react to additive noise (or dc-offsets) and produce a higher noise-floor than that of an  
 353 amplitude-locked loop. This can be shown with a simulation of an ideal amplitude-locked  
 354 loop and ideal Hard Limiter.

355 Consider the case of an FM modulated signal of 2kHz with  $\beta = 5$ . There is no multi-  
 356 path spikes present but additive channel noise has been added which results in an overall  
 357 carrier-to-noise ratio of 17 dB. This is before the onset of thresholding. Figure 13 shows  
 358 a comparison of the IF spectrum at the output of an amplitude-locked loop and hard  
 359 limiter.

360 The amplitude-locked loop noise floor is approximately 9dB down on the equivalent  
 361 limiter noise floor. Thus it is justifiable in using the circuit in replace of a hard limiter in the  
 362 overall system.

363 The amplitude-locked loop recovered carrier output is shown in Fig. 14.

364 In fact the compression of the carrier increases the power at the carrier (of course a hard  
 365 limiter also does this) but with the result of a smaller noise-floor.

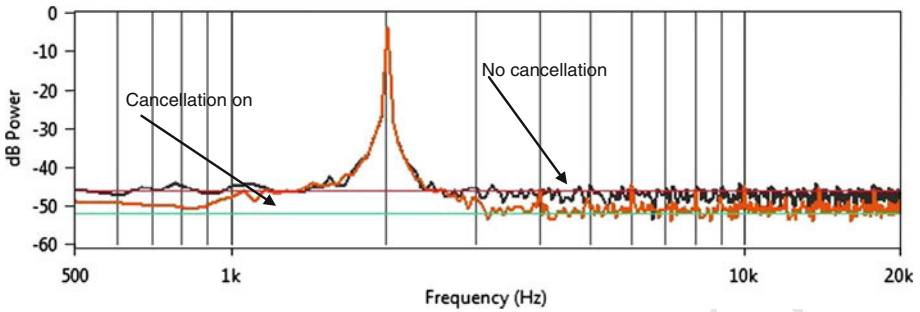


Fig. 15 Effect on baseband noise-floor of cancellation of multipath and noise

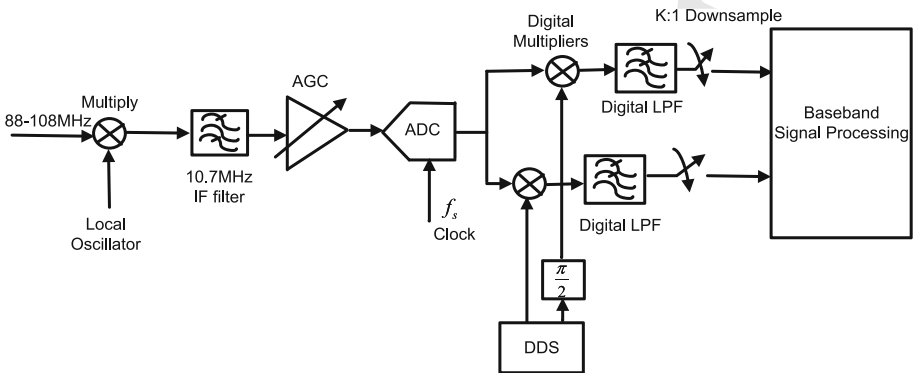


Fig. 16 Software radio architecture

366 The corresponding demodulated output before and after cancellation of the spikes *when*  
 367 *multipath is present* is shown in Fig. 15. The reduction is of course much less than in the  
 368 ideal noise-free case and shows a reduction of 6 dB in the noise-floor after cancellation of  
 369 the spikes.

370 A similar (but not identical) approach was previously shown in [9]. For that paper a  
 371 different method was used to produce the correction term to cancel the spikes and the method  
 372 will not work on multipath propagation. A similar yet different approach was used for co-  
 373 channel interference in Laser Doppler Velocimetry[10]. This is the first time such an approach  
 374 has been applied to multipath FM (Fig. 16).

## 375 6 Software Radio Approach

376 We consider a software approach to the demodulation process. Such an approach is now  
 377 commonplace and finding its way into many real FM radios [11].

378 In this approach the conversion from analogue to digital occurs at IF rather than baseband  
 379 and the down-conversion to baseband is performed digitally including a sample rate reduction.  
 380 The above architecture is free of imbalance problems between I and Q. There is an extension  
 381 of the above architecture whereby the entire FM spectrum is bandlimited (88–108 MHz) by  
 382 a 20 MHz bandpass filter and then sampled and down-converted in a similar manner to the  
 383 above. A sampling rate of 80 MHz is often used for this application and this aliases the original

384 FM band which is centred on 98 MHz down to 18 MHz. This is close to quarter sample rate  
 385 of the converter and gives good separation of the various aliased images. Whichever method  
 386 is used will result in the same end-result which are two components I and Q. For our SCAM-  
 387 FM problem we have an analogue composite FM IF signal (with multipath) from the AGC  
 388 given by:

$$f(t) = r(t) \cos[\omega_c t + \beta \sin(\omega_m t) - \phi(t)] \quad (23)$$

390 To find the I and Q components we first convert the above signal to a sampled signal  
 391 given by

$$f(nT_s) = r(nT_s) \cos[\omega_c nT_s + \beta \sin(\omega_m nT_s) - \phi(nT_s)], \quad n = 0, 1, 2, 3 \dots \quad (24)$$

393 and  $T_s = \frac{1}{f_s}$  is the sampling interval in seconds. For mathematical convenience we drop the  
 394 sampling interval write the above as

$$f(n) = r(n) \cos[\omega_c n + \beta \sin(\omega_m n) - \phi(n)], \quad n = 0, 1, 2, 3 \dots \quad (25)$$

396 We now digitally convert to baseband by multiplying  $f(n)$  by  $\cos(\omega_c n)$  and  $\sin(\omega_c n)$ . This  
 397 gives us after filtering out the  $(2\omega_c n)$  terms:

$$I(n) = r(n) \cos[\beta \sin(\omega_m n) - \phi(n)] \quad (26a)$$

$$Q(n) = r(n) \sin[\beta \sin(\omega_m n) - \phi(n)] \quad (26b)$$

400 which is all that is required for demodulation. A similar result would be obtained using  
 401 any of the other architectures. Down-sampling would normally now occur to lessen the  
 402 computational load but for mathematical purposes of demodulation this need not be used as  
 403 the same result will be obtained with or without a sample rate reduction.

404 The FM demodulated signal which is the digital equivalent of the analogue phase-locked  
 405 loop output is now given by

$$p(n) = \frac{d}{dn} \tan^{-1} \left( \frac{Q(n)}{I(n)} \right) \quad (27)$$

407 This is easily found to be

$$p(n) = \left( \frac{I(n)\dot{Q}(n) - \dot{I}(n)Q(n)}{I^2(n) + Q^2(n)} \right) \quad (28)$$

409 Note that in the above  $I^2(n) + Q^2(n) = r^2(n)$  (from the expressions for I and Q)

410 A number of possible solutions are available to solve the above expressions for  $p(n)$   
 411 including using FIR filters to produce a band-limited differentiator for instance. Here we  
 412 consider a simple solution to show the basic idea. Approximate a differentiator as a first  
 413 difference:

$$\dot{I}(n) = \frac{d}{dn} I(n) \approx I(n) - I(n-1) \quad (29)$$

$$\dot{Q}(n) = \frac{d}{dn} Q(n) \approx Q(n) - Q(n-1) \quad (30)$$

416 Substituting into (28) gives

$$p(n) = \left( \frac{Q(n)I(n-1) - I(n)Q(n-1)}{I^2(n) + Q^2(n)} \right) \quad (31)$$

Author Proof



wondershare™

PDF Editor

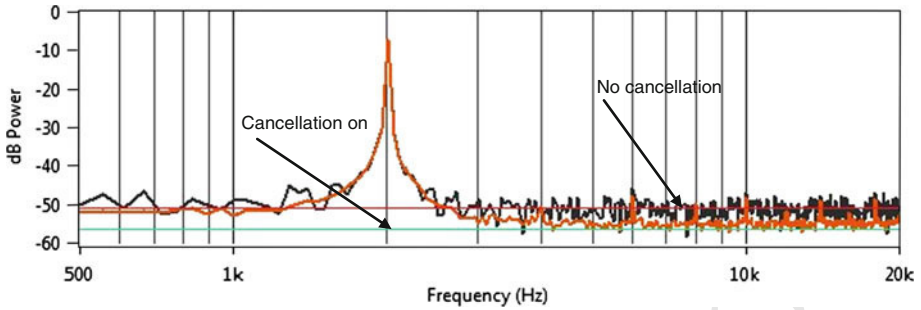


Fig. 17 Software radio: effect on baseband noise-floor of cancellation of multipath and noise

418 To nullify a spike we need to generate the digital equivalent of a spike going to zero at  
 419 the right time (the zero-crossing of the modulating frequency). The analogue correction  
 420 signal is:

$$421 \quad c(t) = \frac{d(t)}{[d(t) + \delta]}$$

422 But since  $d(t) = r^2(t)$  ie the envelope squared which is the same as the AGC output then  
 423 clearly the digital equivalent is

$$424 \quad c(n) = \frac{r^2(n)}{[r^2(n) + \delta]} \quad (32)$$

425 and  $r^2(n) = I^2(n) + Q^2(n)$  is easily found since I and Q are already known.

$$426 \quad c(n) = \frac{I^2(n) + Q^2(n)}{[I^2(n) + Q^2(n) + \delta]} \quad (33)$$

427 The above expression is the digital equivalent of  $c(t)$  and no amplitude-locked loop is  
 428 required.

429 Now considering the same problem as discussed previously (Fig. 15), but now for the  
 430 software radio case (an FM modulated signal of 2 kHz with  $\beta = 5$ . There is multipath present  
 431 and additive channel noise has been added which results in an overall carrier-to-noise ratio  
 432 of 17 dB)

433 It is interesting here to note that the spectrum *before* cancellation in Fig. 17 is equivalent  
 434 in terms of noise-floor as the previous analogue noise-floor case *after* cancellation. An extra  
 435 6 dB reduction in noise-floor is obtained after cancellation using the software approach. This  
 436 indicates a 12 dB reduction with comparison to an analogue signal with no cancellation. Of  
 437 course with the digital receiver the sampling process is considered ideal and no quantization  
 438 noise is modelled in the simulation.

## 439 7 Conclusions

440 A new approach to suppression of multipath noise has been shown which does not involve  
 441 convolutive or adaptive filtering. Both an analogue and software radio architecture has been  
 442 presented which shows that the analogue receiver with canceller is superior in performance  
 443 to one without, and the software approach has the added advantage of a simple solution and

444 even lower noise floor. The method has a wide range of applications mainly in mobile FM  
 445 radio systems where the sound quality is of great concern.

446 **Appendix 1. Simplification of  $\psi(t)$**

447 The difference frequency function is given by (16)

$$448 \quad \psi(t) = \beta \sin(\omega_m(t - \pi/\omega_c)) - \beta \sin(\omega_m t) - \pi \tag{34}$$

449 Now the first sine term in (34) can be written as

$$450 \quad \beta \sin(\omega_m(t - \pi/\omega_c)) = \beta \left[ \sin(\omega_m t) \cos\left(\frac{\pi \omega_m}{\omega_c}\right) - \cos(\omega_m t) \sin\left(\frac{\pi \omega_m}{\omega_c}\right) \right]$$

451 which approximates for small angles of  $k = \frac{\pi \omega_m}{\omega_c}$  to be

$$452 \quad \beta \sin(\omega_m(t - \pi/\omega_c)) \approx \beta \left[ \sin(\omega_m t) \left(1 - \frac{k^2}{2}\right) - k \cos(\omega_m t) \right]$$

453 Adding all terms gives in (34)

$$454 \quad \psi(t) \approx \beta \sin(\omega_m t) - \beta k \cos(\omega_m t) - \beta \sin(\omega_m t) - \frac{k^2}{2} \beta \sin(\omega_m t) - \pi$$

455 OR

$$456 \quad \psi(t) \approx -[\pi + \beta k \cos(\omega_m t)] - \frac{k^2}{2} \beta \sin(\omega_m t)$$

457 Ignoring the second term above as it will be small we get the result

$$458 \quad \psi(t) \approx -(\pi + \beta k \cos(\omega_m t))$$

459 When taking the cosine of  $\psi(t)$  we can simplify accordingly

$$460 \quad \cos \psi(t) \approx \cos[-(\pi + \beta k \cos(\omega_m t))] = -\cos[\beta k \cos(\omega_m t)]$$

461 and this can be further simplified for small angles to be

$$462 \quad \begin{aligned} \cos(\psi(t)) &= -\cos[\beta k \cos(\omega_m t)] = -\left[1 - \frac{1}{2}(\beta k)^2 \cos^2(\omega_m t)\right] \\ 463 \quad &= -\left[1 - \frac{1}{4}(\beta k)^2 [1 + \cos(2\omega_m t)]\right] \\ 464 \quad &= -1 + \frac{1}{4}(\beta k)^2 [1 + \cos(2\omega_m t)] \end{aligned}$$

465 Hence this function is related to twice the modulating frequency. TM

466 **Appendix 2. Differentiation of  $\frac{d}{dt} \tan^{-1} \left[ \frac{m \sin(\psi(t))}{1+m \cos(\psi(t))} \right]$**

467 Recall that the differentiation of  $\frac{d}{dt} \tan^{-1} [f(t)] = \frac{1}{1+[f(t)]^2} f'(t)$  where the shorthand nota-  
 468 tion is used here  $f'(t) = \frac{d}{dt} f(t)$ .

Author Proof



469 To differentiate a function of the form  $\frac{u(t)}{v(t)}$  we use the quotient rule

$$470 \quad \frac{d}{dt} \left( \frac{u(t)}{v(t)} \right) = \frac{v(t)du(t) - u(t)dv(t)}{v^2(t)}$$

471 so that

$$\begin{aligned}
 472 \quad &= \frac{d}{dt} \tan^{-1} \left[ \frac{m \sin(\psi(t))}{1 + m \cos(\psi(t))} \right] \\
 473 \quad &= \left[ \frac{1}{1 + \left\{ \frac{m \sin(\psi(t))}{1 + m \cos(\psi(t))} \right\}^2} \right] \frac{d}{dt} \left[ \frac{m \sin(\psi(t))}{1 + m \cos(\psi(t))} \right] \\
 474 \quad &= \left[ \frac{(1 + m \cos(\psi(t)))^2}{1 + 2m \cos(\psi(t)) + m^2} \right] \frac{d}{dt} \left[ \frac{m \sin(\psi(t))}{1 + m \cos(\psi(t))} \right] \\
 475 \quad &= \left[ \frac{(1 + m \cos(\psi(t)))^2}{1 + 2m \cos(\psi(t)) + m^2} \right] \\
 476 \quad &\times \left[ \frac{(1 + m \cos(\psi(t)))m \cos(\psi(t)) - m \sin(\psi(t))(0 - m \sin(\psi(t)))}{(1 + m \cos(\psi(t)))^2} \right] \frac{d}{dt} \psi(t) \\
 477 \quad &= \left[ \frac{m^2 + m \cos(\psi(t))}{1 + 2m \cos(\psi(t)) + m^2} \right] \frac{d}{dt} \psi(t)
 \end{aligned}$$

478 Now

$$479 \quad \psi(t) = \beta \sin(\omega_m(t - \pi/\omega_c)) - \beta \sin(\omega_m t) - \pi$$

480 so that its derivative is given by

$$481 \quad \frac{d}{dt} \psi(t) = \beta \omega_m [\cos(\omega_m(t - \pi/\omega_c)) - \cos(\omega_m t)]$$

482 hence

$$\begin{aligned}
 483 \quad &\frac{d}{dt} \tan^{-1} \left[ \frac{m \sin(\psi(t))}{1 + m \cos(\psi(t))} \right] \\
 484 \quad &= \left[ \frac{m^2 + m \cos(\psi(t))}{1 + 2m \cos(\psi(t)) + m^2} \right] \beta \omega_m [\cos(\omega_m(t - \pi/\omega_c)) - \cos(\omega_m t)]
 \end{aligned}$$

## 485 References

- 486 1. Corrington, M. S. (1945). Frequency modulation distortion caused by multi-path transmission. *Proceed-*
- 487 *ings of the IRE*, 30, 878–891.
- 488 2. Kammeyer, K. D. (1985). Equalization problems in digital FM receiver. *Signal Processing*, 9, 263–276.
- 489 3. Kammeyer, K. D., Mann, R., & Tobereg, W. (1987). A modified adaptive FIR equalizer for multipath echo
- 490 cancellation in FM transmission. *IEEE Journal, Selected areas of Communications*, SAC-5(2), 226–237.
- 491 4. Tingley-Robert, D. (1997). Reducing multipath fading using adaptive filtering. US Patent application No
- 492 US/08/307300, Filed 16th Sept 1994 issued 9th Dec.
- 493 5. Schnepf, H., Muller, T. & Luy, J.-F. (2001). Channel-diversity in software autoradio. In *Proceedings*
- 494 *vehicular technology conference*, VTC-Spring, Rhodes, Greece.
- 495 6. Treichler, J. R., & Agee, B. G. (1983). A new approach to multipath correction of constant modulus
- 496 signals. *IEEE Transactions on ASSP*, 31(2), 459–472.
- 497 7. Moir, T. J. (1995). Analysis of an amplitude-locked loop. *Electronics Letters*, 31(9), 694–695.
- 498 8. Pettigrew, A. M., & Moir, T. J. (1993). Coherent demodulation of DSSC without pilot tone using the
- 499 amplitude-locked loop. *Journal of the Audio Engineering Society*, 41(12), 998–1007.

- 500 9. Pettigrew, A. M., & Moir, T. J. (1991). Reduction of FM threshold effect by In-band noise cancelling.  
501 *Electronics Letters*, 27(12), 1082–1084.
- 502 10. Clark, D. F., & Moir, T. J. (1999). Application of a PLL and ALL noise reduction process in optical  
503 sensing systems. *IEEE Transactions on Industrial Electronics*, 44(1), 136–138.
- 504 11. Reed, J. H. (2002). Software radio: A modern approach to radio engineering. Englewood Cliffs: Prentice  
505 Hall Professional.

### 506 Author Biographies



**Thomas J. Moir** was born in Dundee Scotland. He was sponsored by GEC Industrial Controls Ltd, Rugby Warwickshire UK from 1976 to 1979 during his B.Sc in control engineering which he was awarded in 1979. In 1983 he received the degree of Ph.D for work on self-tuning filters and controllers. From 1982 to 1983 he was with the Industrial Control unit University of Strathclyde Scotland. From 1983 to 1999 he was a lecturer then senior lecturer at Paisley College/University of Paisley Scotland. Moving to Auckland New-Zealand in 2000, he was with Massey University for 10 years at the Institute of Information and Mathematical Sciences followed by the School of Engineering and Advanced Technology. He moved to AUT University Auckland in 2010 as an associate Professor in the School of Engineering where he works in the area of signal processing and automatic control engineering. He has authored around 100 publication in these fields and is chairman of the Signals and Systems group. He is the holder of one US patent on amplitude-locked loop circuits.



**Archibald M. Pettigrew** was born in Glasgow, Scotland, in 1945. He received the B.Sc degree in electrical engineering from Glasgow University in 1966 and the M.Sc degree in control engineering from Strathclyde University in 1968. He worked first with Ferranti Ltd., Edinburgh on servo design for a laser range-finding system. From 1973 to 1976 he worked as a linear applications engineer with Signetics, Linlithgow. His two specialities were application of phase-locked loops and the Dolby noise-reduction system. In 1976 he joined Burroughs Ltd., Glenrothes, as a design manager responsible for the design of Winchester disk-drive systems. He subsequently was responsible for the design and development of a number of magnetic storage products, namely, floppy-disk drives, magnetic card-readers and cassette tape streamers. From 1986 he worked as a consultant engineer/lecturer at the University of Paisley. In 1990 he formed Ampsys Ltd to further develop work in magnetic recording and the amplitude-locked loop. Mr Pettigrew has filed a large number of patents in disk-drive decoding,

540 data-channel design new methods of audio recording and FM noise reduction methods. He is the holder of  
541 two John Logie Baird awards for innovation and several UK government awards for research. Since 2011 he  
542 has been retired.

wondershare™

# PDF Editor

 Springer